



**HAL**  
open science

## **Pseudomonas aeruginosa LecB suppresses immune responses by inhibiting transendothelial migration**

Janina Sponsel, Yubing Guo, Lutfir Hamzam, Alice Lavanant, Annia Pérez-Riverón, Emma Partiot, Quentin Muller, Julien Rottura, Raphael Gaudin, Dirk Hauck, et al.

### ► To cite this version:

Janina Sponsel, Yubing Guo, Lutfir Hamzam, Alice Lavanant, Annia Pérez-Riverón, et al.. Pseudomonas aeruginosa LecB suppresses immune responses by inhibiting transendothelial migration. EMBO Reports, 2023, 24 (4), pp.e55971. 10.15252/embr.202255971 . hal-04261591

**HAL Id: hal-04261591**










**<https://cnrs.hal.science/hal-04261591>**

Submitted on 15 Nov 2023

**HAL** is a multi-disciplinary open access archive for the deposit and dissemination of scientific research documents, whether they are published or not. The documents may come from teaching and research institutions in France or abroad, or from public or private research centers.

L'archive ouverte pluridisciplinaire **HAL**, est destinée au dépôt et à la diffusion de documents scientifiques de niveau recherche, publiés ou non, émanant des établissements d'enseignement et de recherche français ou étrangers, des laboratoires publics ou privés.

# *Pseudomonas aeruginosa* LecB suppresses immune responses by inhibiting transendothelial migration

Janina Sponse<sup>1,2,3,†</sup>, Yubing Guo<sup>1,2,3,†</sup> , Lutfir Hamzam<sup>1</sup>, Alice C Lavanant<sup>1</sup> , Annia Pérez-Riverón<sup>1</sup>, Emma Partiot<sup>4,5</sup>, Quentin Muller<sup>1,6</sup> , Julien Rottura<sup>1</sup> , Raphael Gaudin<sup>4,5</sup> , Dirk Hauck<sup>7,8,9</sup>, Alexander Titz<sup>7,8,9</sup> , Vincent Flacher<sup>1</sup> , Winfried Römer<sup>2,3,10,\*</sup>  & Christopher G Mueller<sup>1,\*\*</sup> 

## Abstract

*Pseudomonas aeruginosa* is a Gram-negative bacterium causing morbidity and mortality in immuno-compromised humans. It produces a lectin, LecB, that is considered a major virulence factor, however, its impact on the immune system remains incompletely understood. Here we show that LecB binds to endothelial cells in human skin and mice and disrupts the transendothelial passage of leukocytes *in vitro*. It impairs the migration of dendritic cells into the paracortex of lymph nodes leading to a reduced antigen-specific T cell response. Under the effect of the lectin, endothelial cells undergo profound cellular changes resulting in endocytosis and degradation of the junctional protein VE-cadherin, formation of an actin rim, and arrested cell motility. This likely negatively impacts the capacity of endothelial cells to respond to extracellular stimuli and to generate the intercellular gaps for allowing leukocyte diapedesis. A LecB inhibitor can restore dendritic cell migration and T cell activation, underlining the importance of LecB antagonism to reactivate the immune response against *P. aeruginosa* infection.

**Keywords** bacterial lectin; dendritic cells; lymphatics; migration; skin

**Subject Categories** Cell Adhesion, Polarity & Cytoskeleton; Immunology; Microbiology, Virology & Host Pathogen Interaction

**DOI** 10.15252/embr.202255971 | Received 15 August 2022 | Revised 5 February 2023 | Accepted 10 February 2023 | Published online 1 March 2023

**EMBO Reports (2023) 24: e55971**

## Introduction

Lectins, widespread among animals, plants, bacteria, and viruses, are proteins with carbohydrate binding properties (Meiers *et al*, 2019). Microbial lectins play a role in pathogenesis, such as the fimbria lectins FimH and FmlH for *E. coli* infection of the urinary tract (Rosen *et al*, 2008) or the influenza virus hemagglutinin that binds sialic acids of pulmonary epithelial cells (Lewis *et al*, 2022). *P. aeruginosa* is a widespread, Gram-negative bacterium that causes chronic cutaneous wound and airway infections. It belongs to the ESKAPE pathogens and is listed by the World Health Organization as one of the most critical bacterial pathogens. *P. aeruginosa* produces two lectins, LecA and LecB (formerly named PA-IL and PA-III) that form homotetramers and have high affinity for galactose and L-fucose, respectively (Gilboa-Garber, 1972). LecB is noncovalently linked to carbohydrate ligands of the outer bacterial cell surface and can be liberated by interference with soluble sugars or glycans (Tielker *et al*, 2005). It increases bacterial adherence to and infection of epithelial cells of the skin (Landi *et al*, 2019; Thuenauer *et al*, 2020) and the lung and contributes to pathogenicity in mouse models of lung infections (Mewe *et al*, 2005; Chemani *et al*, 2009). In addition, the lectin also contributes to the formation of biofilms (Tielker *et al*, 2005; Diggle *et al*, 2006). Therefore, LecB has been identified as a potential drug target in infections with *P. aeruginosa* (Wagner *et al*, 2016).

During an adaptive immune response against microbial infections, the B cell-driven humoral effector arm generates high-affinity and long-lived immunoglobulins for antibody and complement-mediated cytotoxicity and to block infections of host cells. In parallel, the T cell-mediated effector arm kills infected host cells. The

1 CNRS UPR 3572, IBMC, University of Strasbourg, Strasbourg, France

2 Signalling Research Centers BIOS and CIBSS, University of Freiburg, Freiburg, Germany

3 Faculty of Biology, University of Freiburg, Freiburg, Germany

4 CNRS, Institut de Recherche en Infectiologie de Montpellier (IRIM), Montpellier, France

5 Université de Montpellier, Montpellier, France

6 Laboratoire BIOTIS, Inserm U1026, Université de Bordeaux, Bordeaux, France

7 Chemical Biology of Carbohydrates (CBCH), Helmholtz Institute for Pharmaceutical Research Saarland (HIPS), Helmholtz Centre for Infection Research, Saarbrücken, Germany

8 Deutsches Zentrum für Infektionsforschung (DZIF), Standort Hannover-Braunschweig, Germany

9 Department of Chemistry, Saarland University, Saarbrücken, Germany

10 Freiburg Institute for Advanced Studies (FRIAS), University of Freiburg, Freiburg, Germany

\*Corresponding author. Tel: +33 3 88 41 70 27; E-mail: winfried.roemer@bios.uni-freiburg.de

\*\*Corresponding author. Tel: +49 761 203 67500; E-mail: c.mueller@unistra.fr

†These authors contributed equally to this work

dendritic cells (DCs) are key in initiating an efficacious immune response against bacterial infections. They are professional antigen-presenting cells, migrating from infected tissue via the lymphatic vessels to the draining lymph nodes (LNs), where they present pathogen-derived antigens to activate naïve and memory T cells. Under the influence of environmental cues, DCs direct the polarization of T helper cells supporting the humoral or cell-cytotoxic effector arms.

Microbial lectins, such as LecB, can modulate the immune response through their potent mitogenic potential on immune cells leading to uncontrolled cell proliferation, exhaustion, and cell death (Avichezer & Gilboa-Garber, 1987; Singh & Walia, 2014). LecB and BambL, a L-fucose-binding lectin from *Burkholderia ambifaria*, induce B cell activation and subsequent cell death *in vitro*. Injection of BambL into mice leads to polyclonal activation of B cells (Wilhelm *et al*, 2019; Frensch *et al*, 2021), which could thwart an efficient humoral immune response. However, on the whole, the impact of microbial lectins on the immune system has remained poorly studied.

Here, we investigated the effect of *P. aeruginosa* LecB on the vascular and the immune systems using human skin explants and mouse models. We found that LecB bound to blood and lymphatic endothelial cells *in vitro* and *in vivo* and caused profound cell junctional and cytoskeletal changes, impairing transendothelial migration of leukocytes. LecB inhibits the migration of DCs from skin via the lymphatics into the LN leading to a diminished T cell response, which is restored by a synthetic LecB inhibitor. These findings illustrate how a microbial lectin can curtail an immune response by inhibiting immune cell migration across endothelial barriers.

## Results and Discussion

### LecB disrupts migration of human skin DCs and binds to endothelial cells

To investigate the impact of the *P. aeruginosa* lectins on the immune system, we exposed human skin explants to recombinant LecA and LecB purified from *E. coli* (Chemani *et al*, 2009; Landi *et al*, 2019) for 3 days in culture medium and assessed the spontaneous migration of leukocytes. The cells accumulating in the medium were identified as HLA-DR<sup>-</sup> lymphocytes (mostly memory T cells), epidermal Langerhans cells, dermal CD14<sup>+</sup>, and CD14<sup>-</sup> (CD1a<sup>+</sup>) DCs (Fig 1A). While T cells were not significantly affected by either lectins, there was a significant reduction in dermal CD14<sup>+</sup> and CD14<sup>-</sup> DCs as well as in epidermal Langerhans cells with LecB but not LecA (Fig 1B). Adding the LecB glycomimetic inhibitor DH445 (Sommer *et al*, 2018) restored cell migration (Fig 1C). In light of the role of integrins (ITGs) in leukocyte migration and the loss of ITGb1 from epithelial cells by LecB (Thuenuer *et al*, 2020), we assessed the cell surface expression of CD18/ITGb2, CD11c/ITGaX, and CD11b/ITGaM. There was a reduction in the CD18/ITGb2-CD11c/ITGb2 heterodimer on dermal DCs but not Langerhans cells (Fig EV1). Thus, LecB negatively affects DC migration from human skin by binding to a cellular glycoligand. Given that DCs and Langerhans cells leave tissue via the lymphatic vessels, we next assessed interaction of LecB with the skin lymphatics. To this end, we cultured skin explants for 3 days with LecB conjugated to the

fluorochrome AlexaFluor 488. The skin was then sectioned and stained for CD31 and HLA-DR, expressed by endothelial cells and the dermal DCs/epidermal Langerhans cells, respectively (Fig 1D). There was a noticeable overlap between LecB-A488 and CD31<sup>+</sup> endothelial cells. To confirm the LecB affinity for endothelial cells, the cells were isolated from human skin, expanded and exposed to LecB-A488 in the absence or presence of graded concentrations of the inhibitor DH445. The cells were stained for CD31, CD146, and glycoprotein 38 (podoplanin) and analyzed by flow cytometry (Fig 1E). Both blood and lymphatic endothelial cells bound LecB and the interaction was antagonized with increasing concentrations of DH445. These findings show that treatment with *P. aeruginosa* lectin LecB inhibits the emigration of DCs and binds to human lymphatic and blood endothelial cells.

### The lectin inhibits human leukocyte transmigration *in vitro* and rearranges endothelial cell membrane and cytoskeleton

In light of these findings, we next asked whether LecB inhibits trans-endothelial passage of immune cells. To this end, human CMEC/D3 blood endothelial cells, which form tight cell junctions, were grown as a monolayer on the filter of Transwell plates, and then peripheral blood mononuclear cells (PBMCs), blood-isolated lymphocytes or monocyte were added to the top chamber. The cells were exposed to LecB and migration of the leukocytes across the endothelial cells into the lower chamber was assessed 24 h later (Fig 2A). We found that in the presence of LecB, significantly fewer cells migrated across the endothelial barrier into the lower chamber (Fig 2B). PBMCs and monocytes were most strongly impaired, although CD14<sup>-</sup> lymphocyte transmigration was also significantly decreased. Next, we counted the number of cells remaining on the CMEC/D3 cell monolayer, and, inversely to cell passage, there were more adherent leukocytes in the upper chamber in the presence of LecB (Fig 2C). These findings demonstrate that LecB impairs leukocyte passage across an endothelial monolayer. When staining CMEC/D3 cells for the adherens junctional protein VE-cadherin, we observed that while in untreated conditions, the VE-cadherin was clearly localized at the cell membranes, surprisingly, LecB disrupted this distribution (Fig 2D). We, therefore, analyzed more closely the changes inflicted by LecB on junctional proteins and the cytoskeleton of endothelial cells. First, we determined the binding of LecB-A488 to different endothelial cell lines *in vitro*. The lectin bound to the cell membrane of the human brain microvascular endothelial cell line hCMEC/D3, human umbilical vein endothelial cells (HUVECs), and skin lymphatic cells and was internalized in perinuclear vesicles (Fig EV2A). HUVECs were then left untreated or exposed to LecB for 1 h or 3 h, stained for VE-cadherin, filamentous (F)-actin, focal adhesion kinase (FAK), nuclei were colored with DAPI (Fig 2E), and images quantified for subcellular localization (Fig EV2B). In untreated cells, VE-cadherin was primarily distributed on the cell surface forming adherens junctions, however, in the presence of LecB, location of VE-cadherin shifted into the cytoplasm and was often found in peri-nuclear vesicles. We analyzed VE-cadherin protein levels by western blot and found a time-dependent decrease (Fig 2F). Visualizing F-actin with fluorescent phalloidin uncovered that LecB provoked the reduction in cellular stress fibers and the formation of a cortical actin rim. FAK, which plays a central role in initiating and integrating various signaling pathways with

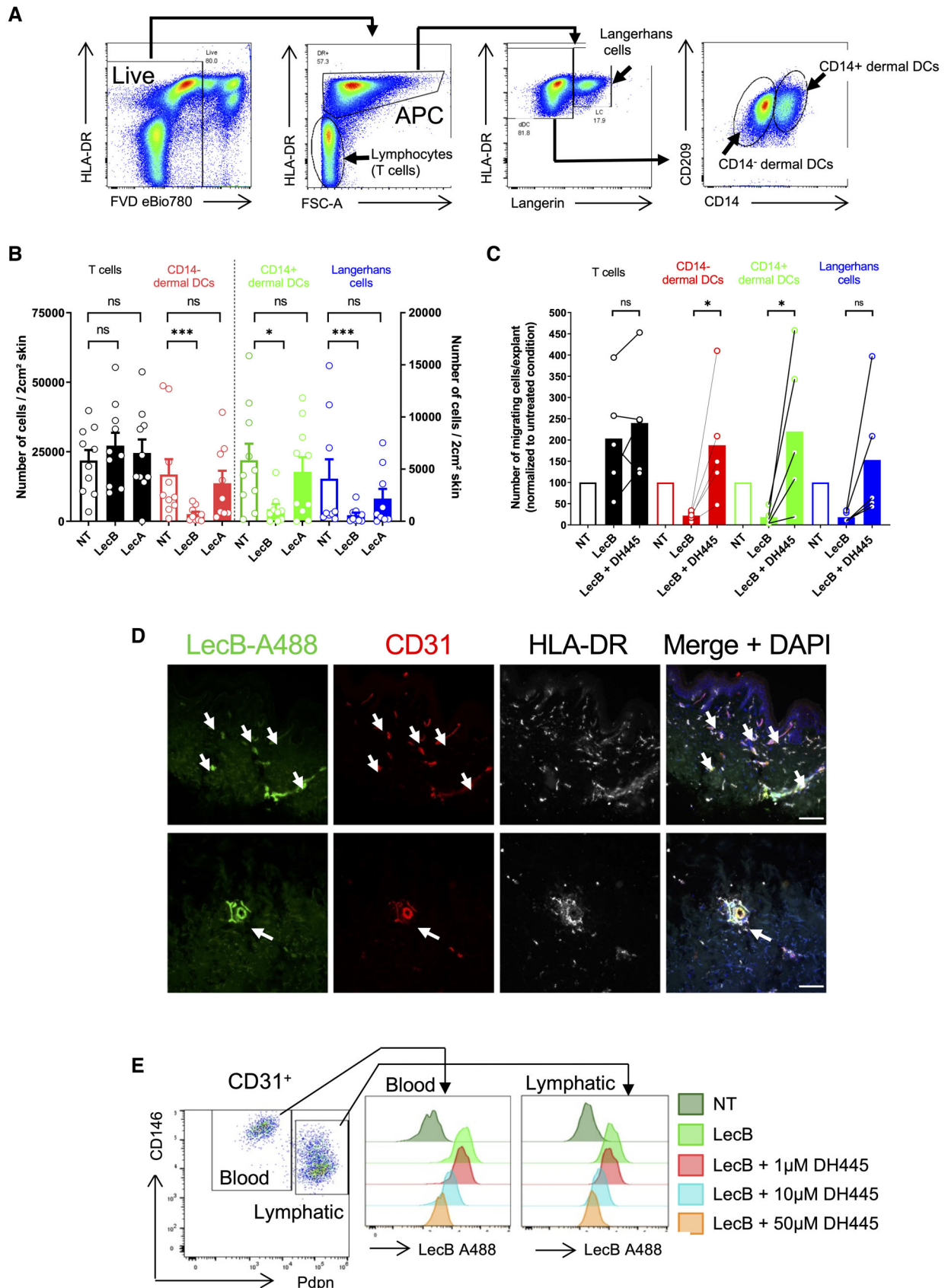


Figure 1.

**Figure 1. LecB binds to endothelial cells in the skin and obstructs cell emigration.**

- A Flow cytometry gating strategy to identify the leukocytes emigrating from human skin explants into cell culture medium.
- B Human skin explants were cultured in complete medium for 3 days in the absence (nontreated, NT) or presence of LecB or LecA, emigrated cells counted and identified by flow cytometry (panel A).
- C As for panel (B) with DH445 and/or LecB added to the culture medium, normalized to the untreated condition.
- D Epifluorescence imaging of human skin cross-sections after incubation of skin explant in culture with LecB-A488 and then stained for CD31, HLA-DR and cell nuclei (DAPI). Arrows point to CD31<sup>+</sup> endothelial cells bound by LecB-A488.
- E Flow cytometry of LecB-A488 binding to ex vivo isolated CD31<sup>+</sup> CD146<sup>+</sup> podoplanin (Pdpn)<sup>-</sup> blood and CD31<sup>+</sup> CD146<sup>-</sup> Pdpn<sup>+</sup> lymphatic endothelial cells in the absence or presence of different concentrations of the LecB inhibitor DH445.

Data information: data are expressed as mean  $\pm$  SEM of individual skin donors, that are linked in (C). The data in (C) are normalized to the untreated (NT) condition. ns, not significant, \* $P < 0.05$ , \*\*\* $P < 0.001$ , as assessed by the Kruskal–Wallis test (B) and Friedman test (C). The scale bars represent 100  $\mu$ m (D).

effect on cytoskeleton (Quadri, 2012), is frequently displaced from a predominantly perimembranous location to an intracellular position after LecB. The alterations in protein expression and localizations were not due to LecB toxicity as assessed by cell viability by MTT and caspase-3 staining (Fig EV3A–C). Given the reduction of actin stress fibers that are central to cell mobility, we performed live imaging of HUVECs with Sir-actin exposed to LecB or left untreated. While untreated cells exhibited actin dynamics concomitant with cell motility, the 3 h LecB treatment left the cells sessile with low levels of polymerized actin (Movies EV1 and EV2). To further explore reduced cell contractility, we determined phosphorylation of the myosin regulatory light chain 2 that stabilizes myosin (Vicente-Manzanares et al, 2009). Western blot showed diminished myosin light chain2 phosphorylation at Ser19, and quantification of immunofluorescence revealed a loss in the perimembranous area after 3 h of LecB exposure (Fig EV3D). In conclusion, LecB reorganizes the VE-cadherin<sup>+</sup> adherens junction and the associated FAK and F-actin cytoskeleton with reduced myosin regulatory light chain phosphorylation, which would have a negative impact on cell contractility and, therefore, on leukocyte diapedesis.

**LecB binds to lymphatic endothelial cells in skin and LN *in vivo***

We next turned to mouse models to explore the functional consequences for the immune system of LecB interaction with endothelial cells. First, LecB-A488 was injected into the ear pinnae of *Prox1<sup>CreERT2</sup> tdTomato<sup>Stop-flox</sup> (iProx-1tdT)* mice that express the red fluorescent tdTomato protein under the *Prox1* promoter active in lymphatic endothelial cells (Bazigou et al, 2011). 4 h later, the ears were split and imaged by confocal microscopy (Fig 3A). LecB-A488 co-localized with the tdTomato<sup>+</sup> lymphatic vessels in addition to binding to other cutaneous structures resembling blood vessels. As lymphatics drain into LNs, we next injected LecB-A488 into the ear pinnae or into the footpad and 4 h later visualized its localization within the auricular and popliteal LNs that respectively drain these injection sites (Fig 3B). LecB bound not only vascular structures, mostly lymphatics expressing both CD31 and CLCA1 and lining the subcapsular and medullary sinuses, but also CD31<sup>+</sup> CLCA1<sup>-</sup> blood vessels. A higher magnification revealed that LecB-A488 labeled structures extending from the subcapsular sinus across the cortex to blood endothelial cells, which are likely conduits transporting lymph-borne material from the lymphatic sinus to high endothelial venules (HEVs) (Gretz et al, 2000). Indeed, in HEVs stained with peripheral node addressins (PNAd), LecB-A488 labeling was apparent on the subluminal side (Fig EV4A). We next examined LecB binding to different cell populations by flow cytometry (Fig 3C).

Lymphatic endothelial cells (LECs), blood endothelial cells (BECs), and fibroblastic reticular cells (FRCs) were identified based on CD31 and gp38 expression, and the HEVs as a PNAd<sup>+</sup> BEC subset. The remaining population that comprises pericytes was noted as double negative (DN). LecB-A488 binding was assessed for each stromal cell population by measuring its mean fluorescence intensity (Fig 3D). We found that LecB primarily targeted LECs, followed by BECs, HEVs, and FRCs. This finding confirms the microscopic assessment of LecB-target cells and supports the conclusion that LecB travels from the skin via the lymphatics to the LNs where it reaches BECs and HEVs via the FRC-formed conduits. We also assessed the mean fluorescence intensity of LecB-A488 in the different hematopoietic cell populations (Fig EV4B–D). The lymphatic sinus-associated macrophages (subcapsular and medullary sinus macrophages, SSM and MSM) displayed the strongest fluorescence followed by other macrophage subsets, whereas DCs showed a much lower binding to LecB. T and B lymphocytes were hardly targeted by the lectin. These data further support the lymphatic draining of subcutaneously injected LecB into the LN, where it is sampled by the lymphatic sinusoidal macrophages.

**LecB interferes with migration of DCs from peripheral tissues and subsequent T cell activation *in vivo***

We next assessed the functional consequences of LecB binding to the lymphatics by assessing DC migration from skin to the LN paracortex, where they prime T cells. First, we determined whether DCs were inhibited by LecB in their migration to LNs by exposing mouse ear skin to the TLR-7 agonist imiquimod (Aldara cream) in the absence or presence of two intradermal injections of LecB. In spite of a strong increase in LN cellularity owing to the inflammatory stimulus, LecB prevented the entry of the migratory skin DC subsets and Langerhans cells into the draining LN (Fig 4A). Similar observations were made when targeting the DEC-205<sup>+</sup> skin DCs (Fig EV5A and B). We then generated DCs from bone marrow precursors (BMDCs), matured by LPS, fluorescently labeled, and injected into ears and footpads of mice treated twice with LecB on one side, while the other side was mock-injected with saline (Fig 4B). In addition, some mice received an intraperitoneal injection of LecB inhibitor DH445. Four days later, the draining auricular and popliteal LNs were recovered, stained for CLCA1<sup>+</sup> lymphatics and B220<sup>+</sup> B cells, and the number of BMDCs associated with lymphatics or localized within the central paracortical T cell zone, devoid of the peripheral B220<sup>+</sup> B cell follicles, was assessed (Fig 4C and D). In the absence of LecB, the majority of BMDCs was found within the paracortex, which was not influenced by DH445. However, in the presence of

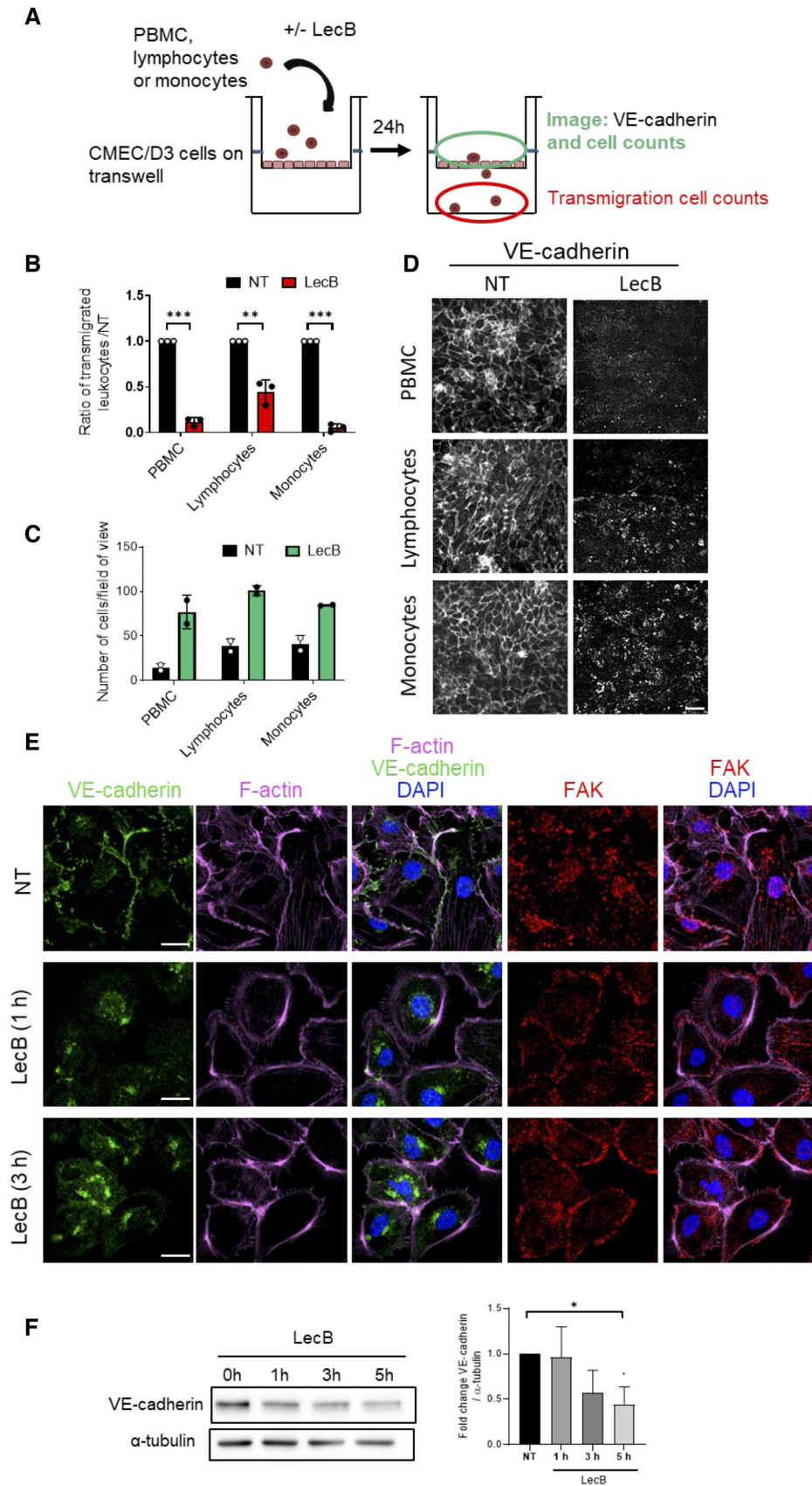


Figure 2.

**Figure 2. LecB restricts leukocyte migration across endothelial cells and inflicts changes to cell membrane and cytoskeleton-associated proteins.**

- A Schematic illustration of the endothelial transmigration assay and its analysis.  
 B The graph shows the number of human peripheral blood mononuclear cells (PBMC), blood-isolated lymphocytes or monocytes transmigrated across the human CMEC/D3 endothelial cell barrier in the presence of LecB, relative to the nontreated (NT) condition.  
 C The graph shows the number of the indicated leukocytes remaining on the endothelial monolayer.  
 D Confocal images of the CMEC/D3 cells stained for VE-cadherin for the indicated experimental conditions.  
 E Confocal images of monolayers of HUVECs, nontreated (NT) or exposed to LecB for 1 or 3 h, were fixed and stained for VE-cadherin, F-actin, focal adhesion kinase (FAK), and nuclei with DAPI.  
 F Left: Western blot analysis of VE-cadherin and  $\alpha$ -tubulin in HUVEC lysates treated with LecB for the indicated times. Right: Densitometric quantification of the western blot of VE-cadherin relative to  $\alpha$ -tubulin.

Data information: (B, F) Data are expressed as mean  $\pm$  SEM,  $n = 3$  biological replicates. \* $P < 0.05$ , \*\* $P < 0.01$ , \*\*\* $P < 0.001$  as assessed by the Student's  $t$ -test (B) Kruskal–Wallis test (F). (C) Data are expressed as mean  $\pm$  SEM,  $n = 2$  biological replicates. The scale bars represent 40  $\mu\text{m}$  (D) and 25  $\mu\text{m}$  (E).

LecB, BMDCs failed to enter the T cell zone and were associated with the subcapsular lymphatics. Strikingly, DH445 reversed LecB-mediated inhibition of BMDC migration into the T cell zone. To determine whether this abnormal migration alters T cell activation, we modified the above experiment by injecting mature BMDCs loaded with ovalbumin into mice having received CFSE-labeled transgenic CD4<sup>+</sup> recognizing an ovalbumin-derived peptide (from OT-II x CD45.1<sup>+</sup> mice) (Fig 4E). The LNs were recovered and the proliferation of CD45.1<sup>+</sup> T cells assessed by dilution of the CFSE label by flow cytometry (Fig 4F). The data, expressed as T cell proliferation, was normalized in each experiment to control mice or mice whose contralateral LN was not exposed to LecB (Fig 4G). We found that LecB significantly reduced T cell proliferation and that this effect was reversed by the LecB inhibitor DH445. Taken together, the data uncovered the ability of LecB to inhibit the generation of an adaptive immune response by restricting DC migration across lymphatics from the periphery to the LN T cell zone.

LecB, produced by the opportunistic bacterium *P. aeruginosa*, is considered a virulence factor, however, its role on the immune system has not been studied. Here, we assessed the consequences of LecB administrated to human skin explants and to mice with respect to immune cell migration and initiation of a T cell immune response. We found that LecB targeted blood and lymphatic endothelial cells in human skin and in mouse skin and LNs. It disrupted the migration of the antigen-presenting cells from the skin via the lymphatics into the LN T cell zone and thereby inhibited the antigen-specific activation of T cells. The lectin restricted transendothelial migration of leukocytes *in vitro* and caused endothelial cell junctional and cytoskeletal changes. These findings support the conclusion that LecB is a potent virulence factor by restraining immune cell trafficking across endothelial barriers and thus preventing the immune system to mount an efficient response.

Immune cell migration is a prerequisite for an efficient immune response by activating T and B cells in the LNs against infections in peripheral tissue. Hereby, DCs play an important role through their capacity to traffic from tissue to LNs linking the innate and the adaptive immune effector arms. After exposing fluorescently tagged LecB intradermally to human skin and the mouse ear, we observed a strong association with blood and lymphatic endothelial cells. Likewise, in the LNs, the lymphatics sinuses were predominantly targeted. Other cells that efficiently bound LecB were the lymphatic sinusoidal macrophages, specialized in sampling and scavenging lymph-borne antigens, blood vessels, and fibroblastic reticular cells that formed the conduits between the LN lymphatic sinus and the HEVs. A molecular basis for the strong interaction of LecB with

endothelial cells may be the glycocalyx, a thick layer of proteoglycans (e.g., syndecans, glypican), glycosaminoglycans, glycoproteins (e.g., selectins, integrins), and glycolipids (Moore *et al*, 2021).

The association of LecB with lymphatics raised the question of its physiological relevance in the context of a bacterial infection. We addressed this by studying leukocyte migration. In humans, Langerhans cells and dermal DC were restricted in their ability to exit the skin into the culture medium. T cells were less affected, indicative of taking a nonlymphatic route. In mice, our data showed that endogenous DCs or injected BMDCs were restrained in entering the LN, which consequently resulted in a lower T cell response. By providing two doses of LecB, we tried to optimize the experimental conditions to anticipate rapid and late BMDC arrival. Yet, because the half-life of LecB interaction with endothelial cells is not known, a more frequent regimen may have been required to observe a complete absence of BMDC migration into the T cell zone and subsequent abrogation of T cell proliferation. Alternatively, the high BMDC numbers may have contributed to overcome LecB-blockage of trans-endothelial migration. The glycomimetic DH445 proved effective in inhibiting LecB effects in skin explants and *in vivo*. DH445, which was administrated intraperitoneally, revealed high potency of inhibition, confirming its advantageous pharmacological properties (Sommer *et al*, 2018). These findings underline DH445 as a promising therapeutic option against *P. aeruginosa*.

We found that LecB-imposed restriction of cell migration from human skin or in mice could be reproduced in an *in vitro* endothelial transmigration assay. The finding that LecB strongly diminished the passage of different types of leukocytes is in line with the notion of general cell alterations rather than modifications of specific receptors or chemotactic signals. By studying HUVECs in more detail, we found that LecB triggered the endocytic degradation of VE-cadherin, changes in FAK subcellular location and the formation of a cortical F-actin rim. How do these changes correlate with reduced leukocyte diapedesis? Leukocytes pass through endothelial barriers mainly via the paracellular route, which involves destabilized cell–cell junctions and active actin stress fibers to create intercellular gaps for cell passage. Endothelial cell barrier enhancement agents lead to the disappearance of central stress fibers to generate a cortical F-actin rim, however, the adherens junctional VE-cadherin is stabilized at the cell surface (Garcia *et al*, 2001; Liu *et al*, 2002; Birukov *et al*, 2004; Birukova *et al*, 2007). One possible explanation for diminished leukocyte transmigration is that LecB impairs leukocyte diapedesis by preventing the development of transcellular tension necessary to create the intercellular openings. This model is supported by loss of stress fibers and reduced myosin regulatory chain phosphorylation,

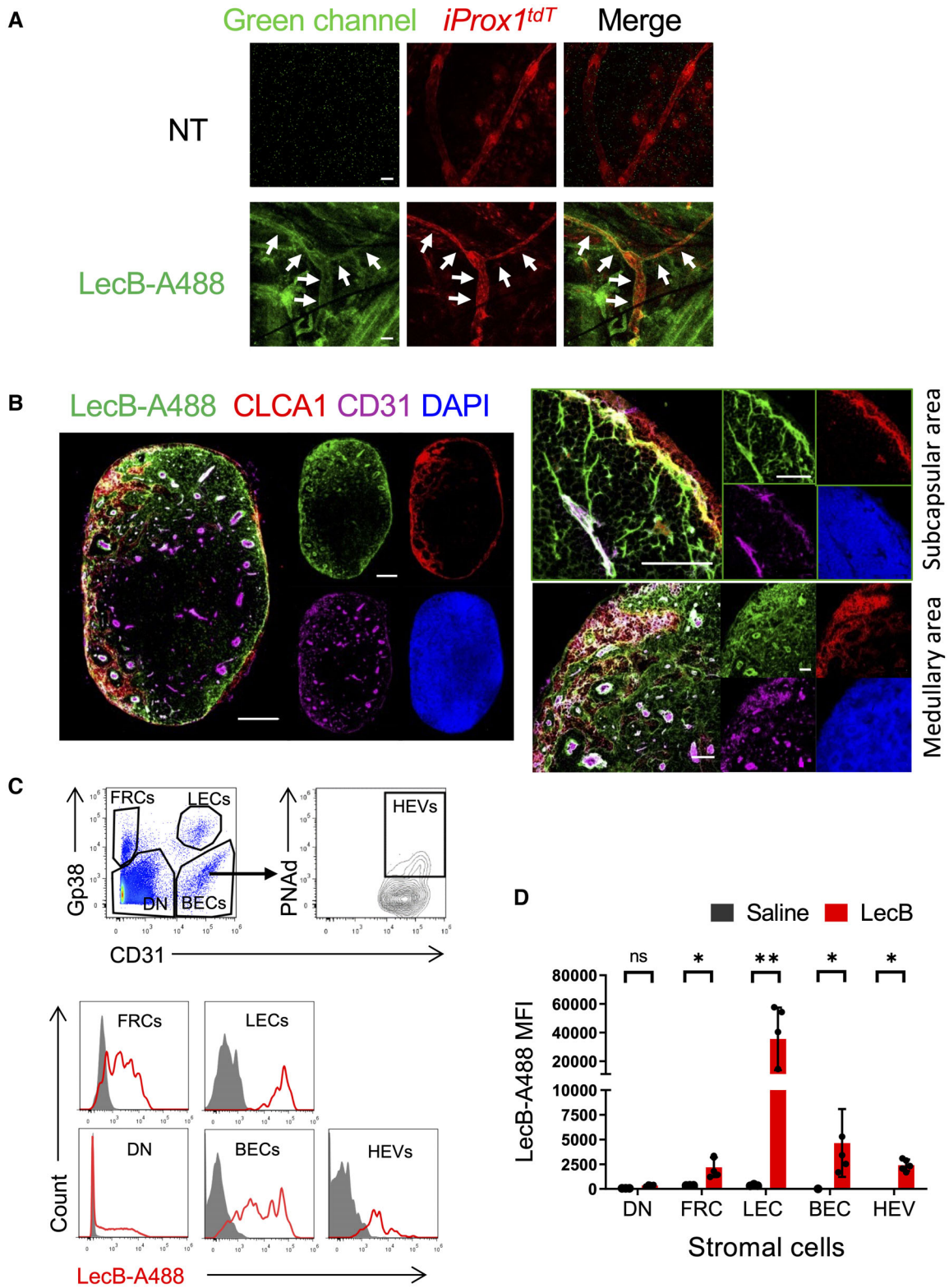


Figure 3.



**Figure 3. Assessment of LecB drainage from the skin to LNs in the mouse.**

- A Whole mount confocal immunofluorescence of ear skin from *Prox1-cre<sup>ERT2</sup> tdTomato<sup>Stop-flox</sup> (iProx1<sup>tdT</sup>)* after injection with LecB-A488 or saline (nontreated, NT). Arrows point to tdTomato+ lymphatic vessels bound by LecB-A488.
- B Confocal imaging of LN sections after LecB-A488 injection and stained for chloride channel calcium-activated 1 (CLCA1), CD31 and cell nuclei (DAPI). Insets on the right show close-ups of the subcapsular and the medullary areas.
- C Top: Flow cytometry gating strategy to identify LN stromal cell subsets among live CD45-TER-119 cells. Bottom: Flow cytometry histograms of green fluorescence for the identified stromal subsets after LecB-A488 (red line) or saline (gray curve) injection.
- D The graph depicts the median fluorescence intensity (MFI) of green fluorescence of LecB-A488 versus saline of the cells analyzed in panel B.
- Data information: The data are expressed as  $\pm$  SEM with each data point represents one biological replicate (two LNs of one mouse). \* $P < 0.05$ , \*\* $P < 0.01$  as determined by the Wilcoxon–Mann–Whitney test. The scale bars represent 50  $\mu$ m (A), 200  $\mu$ m (B left) and 50  $\mu$ m (B right). BEC, blood endothelial cells; DN, double negative cells; FRC, fibroblastic reticular cells; HEV, high endothelial venules; LEC, lymphatic endothelial cells.

which would have a negative impact on cell contractility. However, reduction in integrin cell surface expression by LecB such as CD11c/ITGaX and CD18/ITGb2 may affect migration, although BMDC homing to LNs was not found to be dependent on integrins (Lämmermann *et al*, 2008). Further work is required to clarify the contribution of dysfunctional endothelial cells and compromised leukocyte–endothelial interaction in LecB-mediated inhibition of leukocyte migration.

It has been reported that the second *P. aeruginosa* lectin, LecA, also interacts with endothelial cells (von Bismarck *et al*, 2001; Kirkeby *et al*, 2007). Lectins that have protein homology with *P. aeruginosa* are produced by other bacteria, such as *Burkholderia*, which causes morbidity and mortality among cystic fibrosis patients (Lameignere *et al*, 2008). However, we found that LecA did not inhibit human DC skin emigration, indicating that obstructing leukocyte migration is not a general property of bacterial lectins. An important question is the dynamics of LecB production during an infection and whether it remains associated with the bacterium. Of consideration is also the role of LecB in biofilm formation that may—in the light of our results—protect the bacteria from immunological surveillance and attack. It is also reasonable to assume that the lectins might serve the bacterium to cross the blood or lymphatic endothelial barrier to spread systemically, as previously suggested (Plotkowski *et al*, 1994). In this context, it is interesting to note a case report of *Pseudomonas* in a mediastinal LN in the absence of bacterial counts in the blood, suggesting entry via the lymphatic drainage (Bansal *et al*, 2016). Our study employs purified LecB and calls for further studies using live *P. aeruginosa* expressing or lacking LecB. It also incites further investigation into the immunity-altering impact of other bacterial lectins. LecB inhibitors, similar to DH445, may find an application to bacterial infections beyond *Pseudomonas*.

## Materials and Methods

### Human skin

Fresh abdominal skin was obtained from patients undergoing abdominoplasty with written informed consent and institutional review board approval, in agreement with the Helsinki Declaration and French legislation. 2 cm<sup>2</sup> biopsies of ~ 1 mm thickness were placed at air–liquid interface onto 40- $\mu$ m cell strainers in 6 ml complete medium (RPMI1640 supplemented with 10  $\mu$ g/ml gentamycin, 100 units/ml penicillin, 100  $\mu$ g/ml streptomycin, 10 mM HEPES [all

from Lonza], and 10% fetal calf serum [FCS]). Lec B (5  $\mu$ M) or Lec A (5  $\mu$ M) was added to the skin explants. In some conditions, LecB was preincubated for 30 min with 100  $\mu$ M of DH445 (Sommer *et al*, 2018). Human skin cells that had spontaneously emigrated into the culture medium after 3 days were recovered and stained for HLA-DR, Langerin/CD207, DC-SIGN/CD209 and CD14 (all from BD Pharmingen) to identify CD14<sup>+</sup> and CD14<sup>-</sup> dermal DCs as well as Langerhans cells and T cells. Cells were also stained for the integrin subunits CD18, CD11b, and CD11c (BD Pharmingen).

### Mice

C57BL/6J, CD45.1 (B6.SJL-Ptprca Pepcb/BoyJ), OT-II (B6.Cg-Tg (Tcratcrb)425Cbn/J) (Charles River Laboratories, France), *Prox1-cre<sup>ERT2</sup>* (Bazigou *et al*, 2011), B6;129S6-Gt(ROSA)26Sor<sup>tm9(CAG-tdTomato)Hze</sup> (Jackson Laboratories) mice were kept in pathogen-free conditions. The *Prox1<sup>CreERT2</sup> tdTomato<sup>Stop-flox</sup> (iProx1-1tdT)* mice received 50 mg/kg tamoxifen (Sigma-Aldrich) in sunflower oil/5% ethanol twice with a 24 h interval by gavage 2 weeks before experimentation. The mice then express the red fluorescent tdTomato protein in lymphatics under the specific *Prox1* promoter. All experiments were carried out in conformity with the animal bioethics legislation (APAFIS#16532-2018082814387618v4).

### LecA and LecB preparation

The *P. aeruginosa* lectins were purified from *E. coli* (Chemani *et al*, 2009; Landi *et al*, 2019) using plasmid pET25pa21 (Mitchell *et al*, 2005). LecB was fluorescently labeled with Alexa Fluor488 (LecB-A488) monoreactive NHS ester (Thermo Fisher Scientific) and purified with Zeba Spin desalting columns (Thermo Fisher Scientific) according to manufacturer's instructions.

### Chemical synthesis

The LecB inhibitor *N*- $\beta$ -L-fucopyranosylmethyl 2-thiophenesulfonamide (named here DH445) was synthesized as previously described (Sommer *et al*, 2018).

### Identification of LecB target cells by immunofluorescence of skin and LNs

Human skin (2 cm<sup>2</sup>, 800  $\mu$ m thick) was cultured in RPPMI medium supplemented with 10% fetal calf serum and antibiotics containing 5  $\mu$ g/ml of LecB-A488. After 3 days, the skin was embedded in

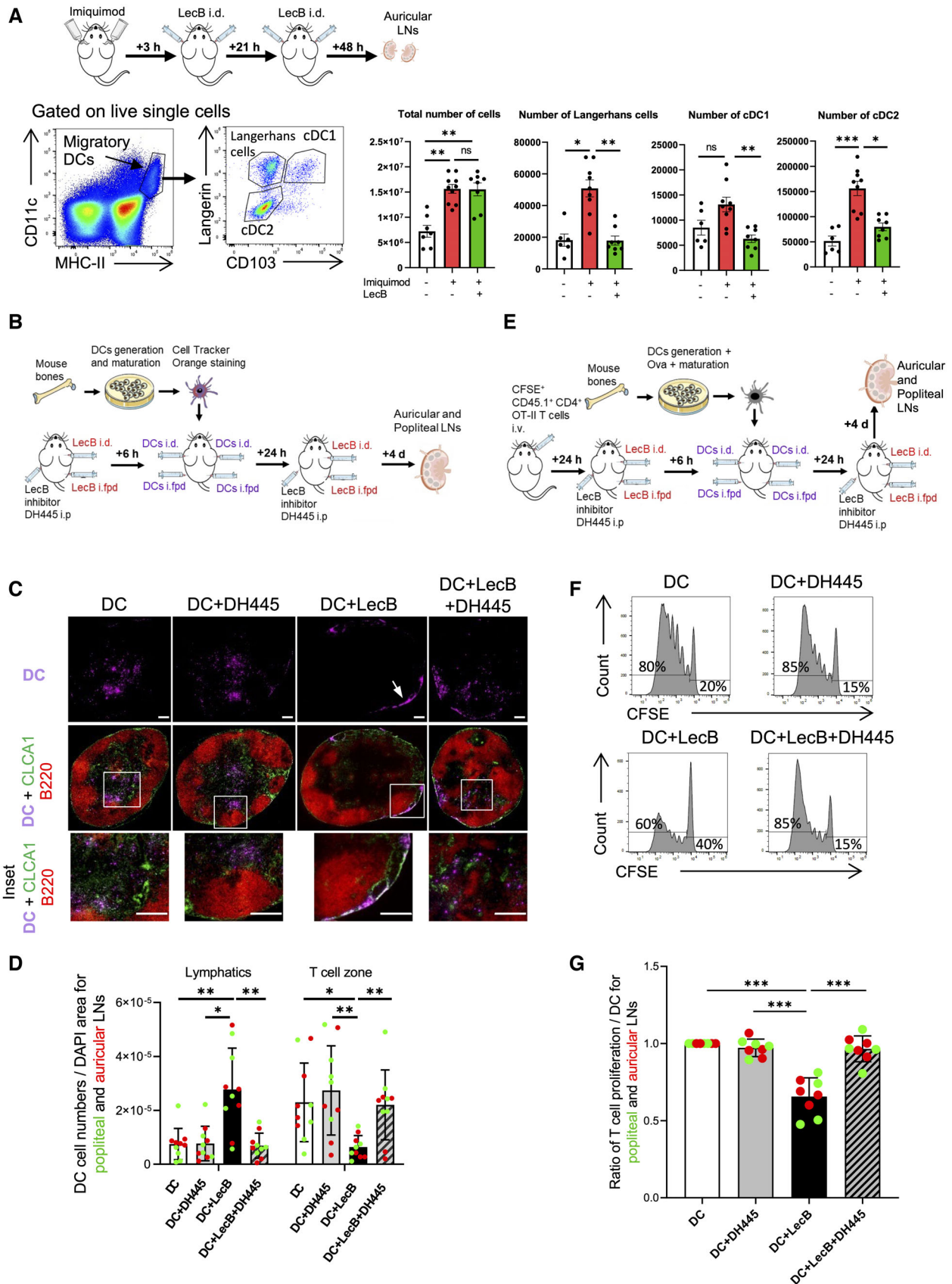


Figure 4.

**Figure 4. Inhibition of DC migration and T cell activation.**

- A Schematic illustration of the experiment to assess inhibition of skin DCs migration to draining auricular LNs by intradermal LecB injection after mobilization by imiquimod (Aldara cream). Left: gating strategy to identify Langerhans cells, cDC1 and cDC2 subsets among the migratory DCs. Right: Graphs depict total auricular LN cell numbers, number of LCs, cDC1, and cDC2 without and with imiquimod application in the absence or presence of LecB.
- B Schematic illustration of the experiment of panels (C, D).
- C Epifluorescent imaging of LN sections stained for chloride channel calcium-activated 1 (CLCA1), expressed by the lymphatic endothelial cells, and B220<sup>+</sup> B cells residing in the LN cortex. DCs are visualized by their Cell Tracker Orange staining. Arrow points to DCs associated with a subcapsular lymphatic sinus. Insets show close-ups of DCs in the T cell paracortex (DC, DC+DH445, DC+LecB+DH445) or in the subcapsular lymphatic sinus (DC+LecB).
- D The graph shows the DC numbers associated with CLCA1<sup>+</sup> lymphatics or the B220<sup>+</sup> T cell zone per LN section normalized for DAPI<sup>+</sup> area.
- E Schematic illustration of the experiment of panels (F, G).
- F Representative flow cytometry profiles of CFSE of donor CD45.1<sup>+</sup> CD3<sup>+</sup> CD4<sup>+</sup> ova-specific T cells in the different recipient mice. The proportion of proliferating versus CFSE<sup>+</sup> undivided T cells is noted.
- G The graph depicts the proportion proliferating T cells of the different experimental condition relative to the DC-only control condition.

Data information: The data are expressed as  $\pm$  SEM with each data point representing (A) two auricular LNs of one mouse, (D, G) a popliteal or an auricular LN of one mouse. \* $P < 0.05$ , \*\* $P < 0.01$ , \*\*\* $P < 0.001$  by (A) Kruskal–Wallis test, (D, G) one-way ANOVA test. Scale bars represent 200  $\mu$ m. cDC1/2, conventional dendritic cells subset 1/2; i.d., intradermal; i.f.p., intrafootpad; i.p., intraperitoneal; LCs, Langerhans cells.

freezing compound (Cell Path, Newton, Poys, UK) and cross-sectioned (7  $\mu$ m thickness). Sections were stained for CD31 and HLA-DR (BD-Pharmingen) and nuclei visualized with DAPI (Sigma-Aldrich). Images were acquired on a Axio Observer.Z1 microscope (Carl Zeiss, Oberkochen, Germany) with a 20 $\times$  air objective (Plan-Apochromat, NA 0.8, DIC, Zeiss) and the Metamorph software (Metamorph, Nashville, TN, USA). Images were processed with the open source software ImageJ. For mice, LecB-A488 (12.5  $\mu$ g) was injected into mouse ear and into the hind footpads. 4 h later, ear pinnae were dissected and the dermal side fixed in 4% paraformaldehyde (PFA) (Sigma-Aldrich) and mounted with Fluoromount-G (Thermo Fisher Scientific). Images were acquired with a confocal microscope (Nikon, Eclipse Ti-E A1R system) and a 20 $\times$  air objective (CFI Plan Fluor 20XC MI, 20 $\times$ /0.75, OFN25 DIC). The auricular and popliteal LNs were harvested, embedded in freezing compound (Cell Path), and cryo-sectioned (8  $\mu$ m thickness). Sections were acetone-fixed and stained for CD169 (BioLegend), chloride channel calcium-activated 1 (CLCA1, clone 10.1.1, a kind gift from Andy Farr, University of Washington, Seattle, USA), CD31 (eBioscience), and anti-PNAd (BioLegend). Nuclei were visualized with DAPI (Sigma-Aldrich).

**Identification of LecB target cells by flow cytometry**

Human skin cells that had spontaneously emigrated into the culture medium after 3 days were recovered and stained for HLA-DR, Langerin/CD207, DC-SIGN/CD209, and CD14 to identify CD14<sup>+</sup> and CD14<sup>-</sup> dermal DCs as well as Langerhans cells and T cells. To isolate blood and lymphatic endothelial cells, human skin was digested with 0.25% trypsin–EDTA (Gibco) to eliminate the epidermis, followed by digestion of the dermis with 1 mg/ml collagenase D (Roche, Switzerland) and 1 mg/ml DNase I (Roche) and for 18 h at 37°C. Endothelial cells were then positively selected using CD31-coupled magnetic beads (Miltenyi Biotec) and amplified in endothelial growth medium (EGM-2, PromoCell) on gelatin-coated flasks (Corning). LecB-A488 (1  $\mu$ g/ml) was added to 5  $\times$  10<sup>4</sup> cells in the absence or presence of the inhibitor DH445 (Sommer *et al*, 2018) (1–50  $\mu$ M) for 2 h before staining cells for CD31 (BioLegend), CD146 (Miltenyi), and Podoplanin (BioLegend). LNs recovered from mice 4 h after injections of 12.5  $\mu$ g LecB-A488 were minced and digested with 1 mg/ml

collagenase D, 1 mg/ml Dispase (Roche) and 0.1 mg/ml DNase I with frequent pipetting until full digestion. The cells were then filtered, red blood cells lysed in ammonium chloride buffer (BioLegend) and incubated with the different antibody cocktails. For stromal cells: anti-CD45-APC/Cy7 (BioLegend), TER-119-APC-eF780 (eBioscience), CD31-PE (BioLegend), anti-gp38/Podoplanin-PE/Cy7 (BioLegend), and anti-PNAd-biotin (BioLegend) followed by streptavidin-APC (eBioscience). DAPI (Sigma-Aldrich) was used to exclude dead cells. For myeloid cells: FcR were blocked with FcR Blocking Reagent (MACS Miltenyi Biotec) and cells stained with anti-CD45-APC/Cy7 (BioLegend), anti-CD11b-PerCP-Cy5.5 (BioLegend), anti-Ly6C-PE (BD Pharmingen), and anti-Ly6G-APC (eBioscience). For sinusoidal macrophages: after FcR-blocking, cells were stained with anti-CD169-PE (BioLegend), anti-CD11c-PE-Cy7 (BD Pharmingen), anti-CD11b-PerCP-Cy5.5 (BioLegend), and anti-F4/80-APC (BioLegend). For DCs: after FcR blocking, cells were stained with anti-CD103-PE (BD Pharmingen), anti-CD11c-PE-Cy7 (BD Pharmingen), and anti-I-A/I-E-AF700 (BioLegend). Cells were washed with PBS and fixed in BD Cytofix™ Fixation Buffer (BD Biosciences) for 20 min and washed in BD Perm/Wash™ Buffer (BD Biosciences) for intracellular staining with Langerin-AF647 (Novus Biologicals). The Fixable Viability Dye eFluor 450 (eBioscience) was used as a dead cell marker. Flow cytometry was done on a Gallios (Beckman Coulter) and data analyzed with the FlowJo software (Tree Star, Inc.).

**Endogenous DC migration**

Mouse ears were treated with Aldara cream, containing 5% imiquimod, and 3 and 21 h later mice received into the ear pinna an injection of 12.5  $\mu$ g LecB in 15  $\mu$ l saline water. For DEC-205 targeting, 1  $\mu$ g anti-DEC-205-A647 antibody diluted in 15  $\mu$ l PBS was injected into ears pinna prior to Aldara cream application (Flacher *et al*, 2012). Auricular LNs were harvested 72 h afterwards. For single cell preparation, LNs were cut into small pieces and digested with 1 mg/ml collagenase D (Roche) and 0.1 mg/ml DNase I (Roche) in RPMI cell culture medium containing 2% FCS for 1 h at 37°C under agitation. For flow cytometry staining the antibodies were: CD11c-PE-Cy7, CD103-PE (BD Pharmingen), MHC-II-AF700, CD205-AF647 (BioLegend), and CD207 (Langerin)-AF488 (Eurobio).

### BMDC generation, migration, and T cell stimulation

Bone marrows were flushed, red blood cells lysed in ammonium chloride buffer (BioLegend), cells filtered and cultured in complete medium containing 25 ng/ml FMS-like tyrosine kinase 3 ligand (hFlt3L, Peprotech). After 8 days, the BMDCs were activated with 100 ng/ml lipopolysaccharide (LPS) for 16 h, harvested and labeled with 15  $\mu$ M Cell Tracker Orange (Thermo Fisher Scientific) for 30 min at 4°C. After washing in PBS,  $2 \times 10^5$  BMDCs were injected subcutaneously into the ear pinna or into the hind footpad of C57BL/6 mice that had received 6 h before on one side 12.5  $\mu$ g LecB into the ear and 12.5  $\mu$ g LecB intra-footpad and contralaterally saline. Some mice concomitantly received a peritoneal injection of 50 mg/kg of LecB inhibitor DH445. After 4 days, the popliteal and auricular LNs were isolated, cryo-sectioned and stained for CLCA1 and B220. The number of Cell Tracker Orange<sup>+</sup> BMDCs trapped within the CLCA1<sup>+</sup> lymphatics or migrated into the B220<sup>-</sup> T cell zone was counted double blindly. For the *in vivo* T cell stimulation assay, BMDCs were generated from C57BL/6 CD45.1<sup>+</sup> bone marrow, and 1  $\mu$ g/ml chicken ovalbumin was added 2 h before addition of LPS. After 18 h, BMDCs were harvested and  $2 \times 10^5$  cells injected into ears and footpads of CD45.2 mice, prepared as described above that had received an intravenous injection of  $10 \times 10^6$  CD4<sup>+</sup> T cells from CD45.1xOT-II F1 mice. The T cells were isolated from spleens and LNs using negative magnetic bead selection (Miltenyi Biotec) and labeled with 500 nM carboxyfluorescein succinimidyl ester (CFSE, Thermo Fisher Scientific) for 15 min at RT. After 4 days, T cell proliferation in the draining LNs was determined by determining the proportion of the CFSE label, successively diluted with each cell division, among the live, CD3<sup>+</sup> CD45.1<sup>+</sup> T cells. Flow cytometry was done on a Gallios (Beckman Coulter) and data analyzed on FlowJo (Tree Star, Inc.).

### Transmigration

Human CMEC/D3 cells (ATCC cell line collection) were grown in 24-well hanging cell culture inserts (PET, 5- $\mu$ m pore, Millipore) at a density of 50,000 cells/cm<sup>2</sup>. Cells were cultured for 7 days prior to transmigration to allow the establishment of a tight monolayer of cells. The tightness of the cell monolayer was verified by transendothelial electrical resistance. PBMCs were isolated from human healthy blood (local blood bank), and monocytes and lymphocytes selected as CD14-microbead-positive (Miltenyi Biotec) and -negative populations, respectively. After Cell Trace Yellow staining (Thermo Fisher Scientific), 250,000 cells were added into the top chamber of the hCMEC/D3 cell-containing inserts in RPMI GlutaMAX (Gibco), supplemented with 2% fetal bovine serum with or without 5  $\mu$ g/ml LecB. The media of the bottom chamber was supplemented with 10% fetal bovine serum. Transwells were kept at 37°C and 5% CO<sub>2</sub> for 17 h and the cells from the bottom chamber were harvested and lysed with CellTiter-Glo Luminescent Cell Viability Assay (Promega). Luminescence was read in 96-well flat bottom white plates (Corning) using the Spark plate reader (Tecan). Cells in the top chamber were fixed with 4% PFA, permeabilized with 0.1% Triton X-100 and 0.5% BSA, and labeled with goat anti human VE-Cadherin (R&D Systems) and a secondary anti-goat antibody coupled with Alexa Fluor 488. Membranes were then detached from the inserts and mounted onto glass slides using Mowiol. Image

acquisition was on an Axio Observer Z1 inverted microscope (Zeiss) equipped with a CSU-X1 spinning disk head (Yokogawa), a back-illuminated Electron-multiplying charge-coupled device (EMCCD) camera (Evolve, Photometrics), and 20 $\times$  (0.75 numerical aperture) air objectives (Zeiss). Images were processed using Fiji (ImageJ software) with the plugin PureDenoise (École polytechnique fédérale de Lausanne, EPFL).

### Endothelial cell–LecB interaction

Human CMEC/D3 cells were grown in EndoGRO-MV Complete Culture Media Kit (Millipore, Burlington, MA, USA), human umbilical vein endothelial cells (HUVECs), and human skin LECs (PromoCell GmbH, Heidelberg, Germany) in endothelial cell growth medium 2 (PromoCell GmbH, Heidelberg, Germany) at 37°C in a humidified incubator containing 5% CO<sub>2</sub> on gelatin-coated plates. Cells at passages 3–6 were used for the experiments. For immunofluorescence, HUVECs were grown on 12-mm glass cover slips in a 4-well Nunc plate (Thermo Fisher Scientific) to 70–100% confluence. Cells were treated with LecB or LecB-A488 (5  $\mu$ g/ml) for 1 and 3 h. Then, cells were fixed with 4% (wt/vol) PFA for 10 min at RT, quenched with 50 mM ammonium chloride and incubated with 0.2% (vol/vol) saponin in PBS. After that, the cells were blocked with 3% BSA (vol/vol) in PBS and subsequently stained with anti-CD144/VE-cadherin (eBioscience) and anti-FAK (D Biosciences), followed by donkey anti-rabbit Alexa488 (Invitrogen) and goat anti-mouse Alexa647 (Invitrogen), respectively. Nuclei and F-actin were stained with DAPI (Sigma-Aldrich) and Phalloidin Alexa565 (Sigma-Aldrich), respectively. Samples were mounted on cover slips using Mowiol medium (Sigma-Aldrich), and images acquired with a Nikon microscopy (Eclipse Ti-E A1R system) with a 60 $\times$  oil immersion objective. Images were processed using Fiji (ImageJ software). Subcellular protein distribution was measured as pixels using Fiji (ImageJ software), drawing the cell's perimembranous and the intracellular areas based on phase contrast images. For the quantification of VE-cadherin, the intercellular pixels/area were subtracted by DAPI pixels/area. For cell viability test, cells were treated with LecB or 1  $\mu$ M Staurosporine (Sigma-Aldrich) for 1 h, followed by 8  $\mu$ M CellEvent Caspase-3/7 Green Detection Reagent (Invitrogen). MTT (3-(4,5-dimethylthiazol-2-yl)-2,5-diphenyltetrazolium bromide) tetrazolium reduction assay kit (Roth, 11465007001) was additionally used.

### Live imaging of HUVECs

HUVECs were seeded on 35-mm imaging dishes with a glass bottom (Ibidi) to 100% confluence. Cells were scratched and treated with or without LecB (5  $\mu$ g/ml) for 3 h at 37°C. Then, cells were washed with PBS twice and incubated with 1 nM SiR-actin (CY-SC001, Spirochrome) for 1 h at 37°C, a fluorogenic, cell permeable dye with high specificity for F-actin. Live images were recorded with a Nikon microscopy (Eclipse Ti-E A1R system) with a 60 $\times$  oil immersion objective for 30 min. Images were processed using Fiji (ImageJ software).

### Western blot

To determine protein expression by western blot, HUVECs were washed, lysed in RIPA buffer containing phosphatase and protease

inhibitors (200  $\mu\text{M}$  pefablock 0.8  $\mu\text{M}$  aprotinin, 11  $\mu\text{M}$  leupeptin, 1% [v/v] phosphatase inhibitor cocktail 3 [Sigma-Aldrich]) for 45 min on ice, and centrifuged to remove cell debris. The protein concentration of the cell lysates was determined using the Pierce BCA Protein Assay Kit (Thermo Scientific) according to the manufacturer's protocol. 25  $\mu\text{g}$  of protein of each sample was separated on 8% SDS-polyacrylamide gels and transferred on nitrocellulose membranes by semi-dry blotting. The membranes were blocked in 3% BSA for 1 h at RT and incubated with VE-cadherin (eBioscience), anti-phospho-myosin light chain2 (Ser19) (Cell Signaling Technology), anti- $\alpha$ -tubulin (Cell Signaling), or anti-GAPDH (Sigma-Aldrich) overnight at 4°C. Membranes were then incubated with anti-rabbit IgG-HRP (Cell Signaling) or anti-mouse IgG-HRP (Cell Signaling) for 1 h at RT. The Clarity western ECL Blotting Substrate (BIO RAD) was used according to the manufacturer's protocol for signal development and chemiluminescence was detected using the Fusion FX chemiluminescence imager (Vilber Lourmat, Marne-la-Vallée, France). Densitometric quantification of blots was performed using ImageJ and protein levels were normalized to  $\alpha$ -tubulin or GAPDH.

### Statistical analysis

Statistical analysis was performed using GraphPad Prism (version 9.0.2) software and the indicated statistical analysis software.

## Data availability

No large primary datasets have been generated and deposited.

**Expanded View** for this article is available [online](#).

### Acknowledgements

This project was supported by the Deutsche Forschungsgemeinschaft (DFG, German Research Foundation) under Germany's Excellence Strategy (EXC-294), by the Deutscher Akademischer Austauschdienst (DAAD, PPP Frankreich 2019 Phase I—project ID: 57445444), by the Ministry for Science, Research and Arts of the State of Baden-Württemberg (Az: 33-7532.20), by the Freiburg Institute for Advanced Studies (FRIAS), the Campus France-Germany Procope programme (42523VF). This work was supported by the Agence Nationale de la Recherche (ANR-20-CE15-0019-01) to RG. JS was supported by an international PhD fellowship from the French Ministry of National Higher Education and Research and a co-doctoral financial aid (No. CT-17-18) from the German-French University. YG acknowledges the China Scholarship Council and a co-doctoral financial aid (No. CT-07-20) from the German-French University. We would like to express our gratitude to the Life Imaging Center (LIC) of the University of Freiburg for support, Jean-Daniel Fauny for help in image data analysis, Delphine Lamon, and Fabien Lhericel for mouse handling and members of the teams for discussions. The funders had no role in study design, data collection and analysis, decision to publish, or preparation of the manuscript. Open Access funding enabled and organized by Projekt DEAL.

### Author contributions

**Janina Sponzel:** Data curation; formal analysis; investigation; methodology; project administration. **Yubing Guo:** Data curation; formal analysis; investigation; methodology. **Lutfir Hamzam:** Investigation; methodology. **Alice C Lavanant:** Data curation; formal analysis; investigation; visualization;

methodology. **Annia Pérez-Riverón:** Data curation; formal analysis; investigation; methodology. **Emma Partiot:** Data curation; investigation; methodology. **Quentin Muller:** Data curation; investigation; methodology. **Julien Rottura:** Investigation; methodology. **Raphael Gaudin:** Conceptualization; resources; supervision; funding acquisition; project administration. **Dirk Hauck:** Resources. **Alexander Titz:** Resources; methodology. **Vincent Flacher:** Conceptualization; data curation; formal analysis; investigation; methodology. **Winfried Römer:** Conceptualization; resources; supervision; funding acquisition; validation; investigation; methodology. **Christopher G Mueller:** Conceptualization; resources; data curation; formal analysis; supervision; funding acquisition; validation; investigation; visualization; methodology; writing – original draft; project administration; writing – review and editing.

### Disclosure and competing interests statement

The authors declare that they have no conflict of interest.

## References

- Avichezer D, Gilboa-Garber N (1987) PA-II, the L-fucose and D-mannose binding lectin of *Pseudomonas aeruginosa* stimulates human peripheral lymphocytes and murine splenocytes. *FEBS Lett* 216: 62–66
- Bansal A, Chand T, Kumar R (2016) *Pseudomonas* species as an uncommon culprit in transbronchial needle aspiration of mediastinal lymph node. *J Assoc Chest Physicians* 4: 91–93
- Bazigou E, Lyons OT, Smith A, Venn GE, Cope C, Brown NA, Makinen T (2011) Genes regulating lymphangiogenesis control venous valve formation and maintenance in mice. *J Clin Invest* 121: 2984–2992
- Birukov KG, Bochkov VN, Birukova AA, Kawkitinarong K, Rios A, Leitner A, Verin AD, Bokoch GM, Leitinger N, Garcia JG (2004) Epoxycyclopentenone-containing oxidized phospholipids restore endothelial barrier function via Cdc42 and Rac. *Circ Res* 95: 892–901
- Birukova AA, Zagranichnaya T, Fu P, Alekseeva E, Chen W, Jacobson JR, Birukov KG (2007) Prostaglandins PGE(2) and PG(2) promote endothelial barrier enhancement via PKA- and Epac1/Rap1-dependent Rac activation. *Exp Cell Res* 313: 2504–2520
- von Bismarck P, Schneppenheim R, Schumacher U (2001) Successful treatment of *Pseudomonas aeruginosa* respiratory tract infection with a sugar solution – a case report on a lectin based therapeutic principle. *Klin Padiatr* 213: 285–287
- Chemani C, Imbert A, de Bentzmann S, Pierre M, Wimmerová M, Guery BP, Faure K (2009) Role of LecA and LecB lectins in *Pseudomonas aeruginosa*-induced lung injury and effect of carbohydrate ligands. *Infect Immun* 77: 2065–2075
- Diggle SP, Stacey RE, Dodd C, Cámara M, Williams P, Winzer K (2006) The galactophilic lectin, LecA, contributes to biofilm development in *Pseudomonas aeruginosa*. *Environ Microbiol* 8: 1095–1104
- Flacher V, Tripp CH, Haid B, Kissenpfennig A, Malissen B, Stoitzner P, Idoyaga J, Romani N (2012) Skin langerin+ dendritic cells transport intradermally injected anti-DEC-205 antibodies but are not essential for subsequent cytotoxic CD8+ T cell responses. *J Immunol* 188: 2146–2155
- Frensch M, Jäger C, Müller PF, Tadić A, Wilhelm I, Wehrum S, Diedrich B, Fischer B, Meléndez AV, Dengjel J et al (2021) Bacterial lectin BambL acts as a B cell superantigen. *Cell Mol Life Sci* 78: 8165–8186
- Garcia JG, Liu F, Verin AD, Birukova A, Dechert MA, Gerthoffer WT, Bamberg JR, English D (2001) Sphingosine 1-phosphate promotes endothelial cell barrier integrity by Edg-dependent cytoskeletal rearrangement. *J Clin Invest* 108: 689–701

- Gilboa-Garber N (1972) Inhibition of broad spectrum hemagglutinin from *Pseudomonas aeruginosa* by D-galactose and its derivatives. *FEBS Lett* 20: 242–244
- Gretz JE, Norbury CC, Anderson AO, Proudfoot AE, Shaw S (2000) Lymph-borne chemokines and other low molecular weight molecules reach high endothelial venules via specialized conduits while a functional barrier limits access to the lymphocyte microenvironments in lymph node cortex. *J Exp Med* 192: 1425–1440
- Kirkeby S, Wimmerová M, Moe D, Hansen AK (2007) The mink as an animal model for *Pseudomonas aeruginosa* adhesion: binding of the bacterial lectins (PA-IL and PA-III) to neoglycoproteins and to sections of pancreas and lung tissues from healthy mink. *Microbes Infect* 9: 566–573
- Lameignere E, Malinová L, Sláviková M, Duchaud E, Mitchell EP, Varrot A, Sedo O, Imberty A, Wimmerová M (2008) Structural basis for mannose recognition by a lectin from opportunistic bacteria *Burkholderia cenocepacia*. *Biochem J* 411: 307–318
- Lämmermann T, Bader BL, Monkley SJ, Worbs T, Wedlich-Söldner R, Hirsch K, Keller M, Förster R, Critchley DR, Fässler R et al (2008) Rapid leukocyte migration by integrin-independent flowing and squeezing. *Nature* 453: 51–55
- Landi A, Mari M, Kleiser S, Wolf T, Gretzmeier C, Wilhelm I, Kiritsi D, Thüner R, Geiger R, Nyström A et al (2019) *Pseudomonas aeruginosa* lectin LecB impairs keratinocyte fitness by abrogating growth factor signalling. *Life Sci Alliance* 2: e201900422
- Lewis AL, Kohler JJ, Aebi M (2022) Microbial lectins: hemagglutinins, Adhesins, and toxins. In *Essentials of Glycobiology*, Varki A, Cummings RD, Esko JD, Stanley P, Hart GW, Aebi M, Mohnen D, Kinoshita T, Packer NH, Prestegard JH et al (eds), pp 505–516. Cold Spring Harbor, NY: Cold Spring Harbor Laboratory Press
- Liu F, Schaphorst KL, Verin AD, Jacobs K, Birukova A, Day RM, Bogatcheva N, Bottaro DP, Garcia JG (2002) Hepatocyte growth factor enhances endothelial cell barrier function and cortical cytoskeletal rearrangement: potential role of glycogen synthase kinase-3beta. *FASEB J* 16: 950–962
- Meiers J, Siebs E, Zahorska E, Titz A (2019) Lectin antagonists in infection, immunity, and inflammation. *Curr Opin Chem Biol* 53: 51–67
- Mewe M, Tielker D, Schönberg R, Schachner M, Jaeger KE, Schumacher U (2005) *Pseudomonas aeruginosa* lectins I and II and their interaction with human airway cilia. *J Laryngol Otol* 119: 595–599
- Mitchell EP, Sabin C, Snajdrová L, Pokorná M, Perret S, Gautier C, Hofr C, Gilboa-Garber N, Koca J, Wimmerová M et al (2005) High affinity fucose binding of *Pseudomonas aeruginosa* lectin PA-III: 1.0 a resolution crystal structure of the complex combined with thermodynamics and computational chemistry approaches. *Proteins* 58: 735–746
- Moore KH, Murphy HA, George EM (2021) The glycocalyx: a central regulator of vascular function. *Am J Physiol Regul Integr Comp Physiol* 320: R508–r518
- Plotkowski MC, Saliba AM, Pereira SH, Cervante MP, Bajolet-Laudinat O (1994) *Pseudomonas aeruginosa* selective adherence to and entry into human endothelial cells. *Infect Immun* 62: 5456–5463
- Quadri SK (2012) Cross talk between focal adhesion kinase and cadherins: role in regulating endothelial barrier function. *Microvasc Res* 83: 3–11
- Rosen DA, Pinkner JS, Walker JN, Elam JS, Jones JM, Hultgren SJ (2008) Molecular variations in *Klebsiella pneumoniae* and *Escherichia coli* FimH affect function and pathogenesis in the urinary tract. *Infect Immun* 76: 3346–3356
- Singh RS, Walia AK (2014) Microbial lectins and their prospective mitogenic potential. *Crit Rev Microbiol* 40: 329–347
- Sommer R, Wagner S, Rox K, Varrot A, Hauck D, Wamhoff E-C, Schreiber J, Ryckmans T, Brunner T, Rademacher C et al (2018) Glycomimetic, orally bioavailable LecB inhibitors block biofilm formation of *Pseudomonas aeruginosa*. *J Am Chem Soc* 140: 2537–2545
- Thuenauer R, Landi A, Trefzer A, Altmann S, Wehrum S, Eierhoff T, Diedrich B, Dengiel J, Nyström A, Imberty A et al (2020) The *Pseudomonas aeruginosa* lectin LecB causes integrin internalization and inhibits epithelial wound healing. *mBio* 11: e03260-19
- Tielker D, Hacker S, Loris R, Strathmann M, Wingender J, Wilhelm S, Rosenau F, Jaeger KE (2005) *Pseudomonas aeruginosa* lectin LecB is located in the outer membrane and is involved in biofilm formation. *Microbiology* 151: 1313–1323
- Vicente-Manzanares M, Ma X, Adelstein RS, Horwitz AR (2009) Non-muscle myosin II takes Centre stage in cell adhesion and migration. *Nat Rev Mol Cell Biol* 10: 778–790
- Wagner S, Sommer R, Hinsberger S, Lu C, Hartmann RW, Empting M, Titz A (2016) Novel strategies for the treatment of *Pseudomonas aeruginosa* infections. *J Med Chem* 59: 5929–5969
- Wilhelm I, Levit-Zerdoun E, Jakob J, Villringer S, Frensch M, Übelhart R, Landi A, Müller P, Imberty A, Thuenauer R et al (2019) Carbohydrate-dependent B cell activation by fucose-binding bacterial lectins. *Sci Signal* 12: eaao7194



**License:** This is an open access article under the terms of the [Creative Commons Attribution-NonCommercial-NoDerivs](https://creativecommons.org/licenses/by-nc-nd/4.0/) License, which permits use and distribution in any medium, provided the original work is properly cited, the use is non-commercial and no modifications or adaptations are made.